

Contents lists available at [SciVerse ScienceDirect](http://SciVerse.ScienceDirect.com)

Physics Letters B

www.elsevier.com/locate/physletbSearch for anomalous Wtb couplings in single top quark production in $p\bar{p}$ collisions at $\sqrt{s} = 1.96$ TeV

D0 Collaboration

V.M. Abazov^{ah}, B. Abbott^{bt}, B.S. Acharya^{ab}, M. Adams^{av}, T. Adams^{at}, G.D. Alexeev^{ah}, G. Alkhazov^{al}, A. Alton^{bh,1}, G. Alverson^{bg}, G.A. Alves^b, M. Aoki^{au}, A. Askew^{at}, B. Åsman^{an}, S. Atkins^{be}, O. Atramentov^{bl}, K. Augstenⁱ, C. Avila^g, J. BackusMayes^{ca}, F. Badaud^l, L. Bagby^{au}, B. Baldin^{au}, D.V. Bandurin^{at}, S. Banerjee^{ab}, E. Barberis^{bg}, P. Baringer^{bc}, J. Barreto^c, J.F. Bartlett^{au}, U. Bassler^q, V. Bazterra^{av}, A. Bean^{bc}, M. Begalli^c, C. Belanger-Champagne^{an}, L. Bellantoni^{au}, S.B. Beri^z, G. Bernardi^p, R. Bernhard^u, I. Bertram^{ao}, M. Besançon^q, R. Beuselinck^{ap}, V.A. Bezzubov^{ak}, P.C. Bhat^{au}, V. Bhatnagar^z, G. Blazey^{aw}, S. Blessing^{at}, K. Bloom^{bk}, A. Boehnlein^{au}, D. Boline^{bq}, E.E. Boos^{aj}, G. Borissov^{ao}, T. Bose^{bf}, A. Brandt^{bw}, O. Brandt^v, R. Brock^{bi}, G. Brooijmans^{bo}, A. Bross^{au}, D. Brown^p, J. Brown^p, X.B. Bu^{au}, M. Buehler^{au}, V. Buescher^w, V. Bunichev^{aj}, S. Burdin^{ao,2}, T.H. Burnett^{ca}, C.P. Buszello^{an}, B. Calpasⁿ, E. Camacho-Pérez^{ae}, M.A. Carrasco-Lizarraga^{bc}, B.C.K. Casey^{au}, H. Castilla-Valdez^{ae}, S. Chakrabarti^{bq}, D. Chakraborty^{aw}, K.M. Chan^{ba}, A. Chandra^{by}, E. Chapon^q, G. Chen^{bc}, S. Chevalier-Théry^q, D.K. Cho^{bv}, S.W. Cho^{ad}, S. Choi^{ad}, B. Choudhary^{aa}, S. Cihangir^{au}, D. Claes^{bk}, J. Clutter^{bc}, M. Cooke^{au}, W.E. Cooper^{au}, M. Corcoran^{by}, F. Couderc^q, M.-C. Cousinouⁿ, A. Croc^q, D. Cutts^{bv}, A. Das^{ar}, G. Davies^{ap}, K. De^{bw}, S.J. de Jong^{ag}, E. De La Cruz-Burelo^{ae}, F. Déliot^q, R. Demina^{bp}, D. Denisov^{au}, S.P. Denisov^{ak}, S. Desai^{au}, C. Deterre^q, K. DeVaughan^{bk}, H.T. Diehl^{au}, M. Diesburg^{au}, P.F. Ding^{aq}, A. Dominguez^{bk}, T. Dorland^{ca}, A. Dubey^{aa}, L.V. Dudko^{aj}, D. Duggan^{bl}, A. Duperrinⁿ, S. Dutt^z, A. Dyshkant^{aw}, M. Eads^{bk}, D. Edmunds^{bi}, J. Ellison^{as}, V.D. Elvira^{au}, Y. Enari^p, H. Evans^{ay}, A. Evdokimov^{br}, V.N. Evdokimov^{ak}, G. Facini^{bg}, T. Ferbel^{bp}, F. Fiedler^w, F. Filthaut^{ag}, W. Fisher^{bi}, H.E. Fisk^{au}, M. Fortner^{aw}, H. Fox^{ao}, S. Fuess^{au}, A. Garcia-Bellido^{bp}, G.A. García-Guerra^{ae,3}, V. Gavrilov^{ai}, P. Gay^l, W. Geng^{n,bi}, D. Gerbaudo^{bm}, C.E. Gerber^{av}, Y. Gershtein^{bl}, G. Ginther^{au,bp}, G. Golovanov^{ah}, A. Goussiou^{ca}, P.D. Grannis^{bq}, S. Greder^r, H. Greenlee^{au}, Z.D. Greenwood^{be}, E.M. Gregores^d, G. Grenier^s, Ph. Gris^l, J.-F. Grivaz^o, A. Grohsjean^q, S. Grünendahl^{au}, M.W. Grünewald^{ac}, T. Guillemin^o, G. Gutierrez^{au}, P. Gutierrez^{bt}, A. Haas^{bo,4}, S. Hagopian^{at}, J. Haley^{bg}, L. Han^f, K. Harder^{aq}, A. Harel^{bp}, J.M. Hauptman^{bb}, J. Hays^{ap}, T. Head^{aq}, T. Hebbeker^t, D. Hedin^{aw}, H. Hegab^{bu}, A.P. Heinson^{as}, U. Heintz^{bv}, C. Hensel^v, I. Heredia-De La Cruz^{ae}, K. Herner^{bh}, G. Hesketh^{aq,5}, M.D. Hildreth^{ba}, R. Hirosky^{bz}, T. Hoang^{at}, J.D. Hobbs^{bq}, B. Hoeneisen^k, M. Hohlfeld^w, Z. Hubacek^{i,q}, V. Hynekⁱ, I. Iashvili^{bn}, Y. Ilchenko^{bx}, R. Illingworth^{au}, A.S. Ito^{au}, S. Jabeen^{bv}, M. Jaffré^o, D. Jaminⁿ, A. Jayasinghe^{bt}, R. Jesik^{ap}, K. Johns^{ar}, M. Johnson^{au}, A. Jonckheere^{au}, P. Jonsson^{ap}, J. Joshi^z, A.W. Jung^{au}, A. Juste^{am}, K. Kaadze^{bd}, E. Kajfaszⁿ, D. Karmanov^{aj}, P.A. Kasper^{au}, I. Katsanos^{bk}, R. Kehoe^{bx}, S. Kermicheⁿ, N. Khalatyan^{au}, A. Khanov^{bu}, A. Kharchilava^{bn}, Y.N. Kharzheev^{ah}, J.M. Kohli^z, A.V. Kozelov^{ak}, J. Kraus^{bi}, S. Kulikov^{ak}, A. Kumar^{bn}, A. Kupco^j, T. Kurča^s, V.A. Kuzmin^{aj}, J. Kvita^h, S. Lammers^{ay}, G. Landsberg^{bv}, P. Lebrun^s, H.S. Lee^{ad}, S.W. Lee^{bb}, W.M. Lee^{au}, J. Lellouch^p, L. Li^{as}, Q.Z. Li^{au}, S.M. Lietti^e, J.K. Lim^{ad}, D. Lincoln^{au}, J. Linnemann^{bi}, V.V. Lipaev^{ak}, R. Lipton^{au}, Y. Liu^f, A. Lobodenko^{al}, M. Lokajicek^j, R. Lopes de Sa^{bq}, H.J. Lubatti^{ca}, R. Luna-Garcia^{ae,6}, A.L. Lyon^{au}, A.K.A. Maciel^b, D. Mackin^{by}, R. Madar^q, R. Magaña-Villalba^{ae}, S. Malik^{bk}, V.L. Malyshev^{ah}, Y. Maravin^{bd}, J. Martínez-Ortega^{ae}, R. McCarthy^{bq}, C.L. McGivern^{bc}, M.M. Meijer^{ag}, A. Melnitchouk^{bj}, D. Menezes^{aw}, P.G. Mercadante^d, M. Merkin^{aj}, A. Meyer^t, J. Meyer^v, F. Miconi^r, N.K. Mondal^{ab}, G.S. Muanzaⁿ, M. Mulhearn^{bz}, E. Nagyⁿ, M. Naimuddin^{aa}, M. Narain^{bv}, R. Nayyar^{aa}, H.A. Neal^{bh},

J.P. Negret^g, P. Neustroev^{al}, S.F. Novaes^e, T. Nunnemann^x, G. Obrant^{al,†}, J. Orduna^{by}, N. Osmanⁿ, J. Osta^{ba}, G.J. Otero y Garzón^a, M. Padilla^{as}, A. Pal^{bw}, N. Parashar^{az}, V. Parihar^{bv}, S.K. Park^{ad}, R. Partridge^{bv,4}, N. Parua^{ay}, A. Patwa^{br}, B. Penning^{au}, M. Perfilov^{aj}, Y. Peters^{aq}, K. Petridis^{aq}, G. Petrillo^{bp}, P. Pétroff^o, R. Piegaia^a, M.-A. Pleier^{br}, P.L.M. Podesta-Lerma^{ae,7}, V.M. Podstavkov^{au}, P. Polozov^{ai}, A.V. Popov^{ak}, M. Prewitt^{by}, D. Price^{ay}, N. Prokopenko^{ak}, J. Qian^{bh}, A. Quadt^v, B. Quinn^{bj}, M.S. Rangel^b, K. Ranjan^{aa}, P.N. Ratoff^{ao}, I. Razumov^{ak}, P. Renkel^{bx}, M. Rijssenbeek^{bq}, I. Ripp-Baudot^r, F. Rizatdinova^{bu}, M. Rominsky^{au}, A. Ross^{ao}, C. Royon^q, P. Rubinov^{au}, R. Ruchti^{ba}, G. Safronov^{ai}, G. Sajot^m, P. Salcido^{aw}, A. Sánchez-Hernández^{ae}, M.P. Sanders^x, B. Sanghi^{au}, A.S. Santos^e, G. Savage^{au}, L. Sawyer^{be}, T. Scanlon^{ap}, R.D. Schamberger^{bq}, Y. Scheglov^{al}, H. Schellman^{ax}, T. Schliephake^y, S. Schlobohm^{ca}, C. Schwanenberger^{aq}, R. Schwienhorst^{bi}, J. Sekaric^{bc}, H. Severini^{bt}, E. Shabalina^v, V. Shary^q, A.A. Shchukin^{ak}, R.K. Shivpuri^{aa}, V. Simakⁱ, V. Sirotenko^{au}, P. Skubic^{bt}, P. Slattery^{bp}, D. Smirnov^{ba}, K.J. Smith^{bn}, G.R. Snow^{bk}, J. Snow^{bs}, S. Snyder^{br}, S. Söldner-Rembold^{aq}, L. Sonnenschein^t, K. Soustruznik^h, J. Stark^m, V. Stolin^{ai}, D.A. Stoyanova^{ak}, M. Strauss^{bt}, D. Strom^{av}, L. Stutte^{au}, L. Suter^{aq}, P. Svoisky^{bt}, M. Takahashi^{aq}, A. Tanasijczuk^a, M. Titov^q, V.V. Tokmenin^{ah}, Y.-T. Tsai^{bp}, K. Tschann-Grimm^{bq}, D. Tsybychev^{bq}, B. Tuchming^q, C. Tully^{bm}, L. Uvarov^{al}, S. Uvarov^{al}, S. Uzunyan^{aw}, R. Van Kooten^{ay}, W.M. van Leeuwen^{af}, N. Varelas^{av}, E.W. Varnes^{ar}, I.A. Vasilyev^{ak}, P. Verdier^s, L.S. Vertogradov^{ah}, M. Verzocchi^{au}, M. Vesterinen^{aq}, D. Vilanova^q, P. Vokacⁱ, H.D. Wahl^{at}, M.H.L.S. Wang^{au}, J. Warchol^{ba}, G. Watts^{ca}, M. Wayne^{ba}, M. Weber^{au,8}, L. Welty-Rieger^{ax}, A. White^{bw}, D. Wicke^y, M.R.J. Williams^{ao}, G.W. Wilson^{bc}, M. Wobisch^{be}, D.R. Wood^{bg}, T.R. Wyatt^{aq}, Y. Xie^{au}, R. Yamada^{au}, W.-C. Yang^{aq}, T. Yasuda^{au}, Y.A. Yatsunenkov^{ah}, Z. Ye^{au}, H. Yin^{au}, K. Yip^{br}, S.W. Youn^{au}, J. Yu^{bw}, T. Zhao^{ca}, B. Zhou^{bh}, J. Zhu^{bh}, M. Zielinski^{bp}, D. Zieminska^{ay}, L. Zivkovic^{bv}

^a Universidad de Buenos Aires, Buenos Aires, Argentina

^b LAFEX, Centro Brasileiro de Pesquisas Físicas, Rio de Janeiro, Brazil

^c Universidade do Estado do Rio de Janeiro, Rio de Janeiro, Brazil

^d Universidade Federal do ABC, Santo André, Brazil

^e Instituto de Física Teórica, Universidade Estadual Paulista, São Paulo, Brazil

^f University of Science and Technology of China, Hefei, People's Republic of China

^g Universidad de los Andes, Bogotá, Colombia

^h Charles University, Faculty of Mathematics and Physics, Center for Particle Physics, Prague, Czech Republic

ⁱ Czech Technical University in Prague, Prague, Czech Republic

^j Center for Particle Physics, Institute of Physics, Academy of Sciences of the Czech Republic, Prague, Czech Republic

^k Universidad San Francisco de Quito, Quito, Ecuador

^l LPC, Université Blaise Pascal, CNRS/IN2P3, Clermont, France

^m LPSC, Université Joseph Fourier Grenoble 1, CNRS/IN2P3, Institut National Polytechnique de Grenoble, Grenoble, France

ⁿ CPPM, Aix-Marseille Université, CNRS/IN2P3, Marseille, France

^o LAL, Université Paris-Sud, CNRS/IN2P3, Orsay, France

^p LPNHE, Universités Paris VI and VII, CNRS/IN2P3, Paris, France

^q CEA, Ifre, SPP, Saclay, France

^r IPHC, Université de Strasbourg, CNRS/IN2P3, Strasbourg, France

^s IPNL, Université Lyon 1, CNRS/IN2P3, Villeurbanne, France and Université de Lyon, Lyon, France

^t III. Physikalisches Institut A, RWTH Aachen University, Aachen, Germany

^u Physikalisches Institut, Universität Freiburg, Freiburg, Germany

^v II. Physikalisches Institut, Georg-August-Universität Göttingen, Göttingen, Germany

^w Institut für Physik, Universität Mainz, Mainz, Germany

^x Ludwig-Maximilians-Universität München, München, Germany

^y Fachbereich Physik, Bergische Universität Wuppertal, Wuppertal, Germany

^z Panjab University, Chandigarh, India

^{aa} Delhi University, Delhi, India

^{ab} Tata Institute of Fundamental Research, Mumbai, India

^{ac} University College Dublin, Dublin, Ireland

^{ad} Korea Detector Laboratory, Korea University, Seoul, Republic of Korea

^{ae} CINVESTAV, Mexico City, Mexico

^{af} Nikhef, Science Park, Amsterdam, The Netherlands

^{ag} Radboud University Nijmegen, Nijmegen, and Nikhef, Science Park, Amsterdam, The Netherlands

^{ah} Joint Institute for Nuclear Research, Dubna, Russia

^{ai} Institute for Theoretical and Experimental Physics, Moscow, Russia

^{aj} Moscow State University, Moscow, Russia

^{ak} Institute for High Energy Physics, Protvino, Russia

^{al} Petersburg Nuclear Physics Institute, St. Petersburg, Russia

^{am} Institució Catalana de Recerca i Estudis Avançats (ICREA) and Institut de Física d'Altes Energies (IFAE), Barcelona, Spain

^{an} Stockholm University, Stockholm and Uppsala University, Uppsala, Sweden

^{ao} Lancaster University, Lancaster LA1 4YB, United Kingdom

^{ap} Imperial College London, London SW7 2AZ, United Kingdom

^{aq} The University of Manchester, Manchester M13 9PL, United Kingdom

^{ar} University of Arizona, Tucson, AZ 85721, USA

^{as} University of California Riverside, Riverside, CA 92521, USA

^{at} Florida State University, Tallahassee, FL 32306, USA

- ^{au} Fermi National Accelerator Laboratory, Batavia, IL 60510, USA
^{av} University of Illinois at Chicago, Chicago, IL 60607, USA
^{aw} Northern Illinois University, DeKalb, IL 60115, USA
^{ax} Northwestern University, Evanston, IL 60208, USA
^{ay} Indiana University, Bloomington, IN 47405, USA
^{az} Purdue University Calumet, Hammond, IN 46323, USA
^{ba} University of Notre Dame, Notre Dame, IN 46556, USA
^{bb} Iowa State University, Ames, IA 50011, USA
^{bc} University of Kansas, Lawrence, KS 66045, USA
^{bd} Kansas State University, Manhattan, KS 66506, USA
^{be} Louisiana Tech University, Ruston, LA 71272, USA
^{bf} Boston University, Boston, MA 02215, USA
^{bg} Northeastern University, Boston, MA 02115, USA
^{bh} University of Michigan, Ann Arbor, MI 48109, USA
^{bi} Michigan State University, East Lansing, MI 48824, USA
^{bj} University of Mississippi, University, MS 38677, USA
^{bk} University of Nebraska, Lincoln, NE 68588, USA
^{bl} Rutgers University, Piscataway, NJ 08855, USA
^{bm} Princeton University, Princeton, NJ 08544, USA
^{bn} State University of New York, Buffalo, NY 14260, USA
^{bo} Columbia University, New York, NY 10027, USA
^{bp} University of Rochester, Rochester, NY 14627, USA
^{bq} State University of New York, Stony Brook, NY 11794, USA
^{br} Brookhaven National Laboratory, Upton, NY 11973, USA
^{bs} Langston University, Langston, OK 73050, USA
^{bt} University of Oklahoma, Norman, OK 73019, USA
^{bu} Oklahoma State University, Stillwater, OK 74078, USA
^{bv} Brown University, Providence, RI 02912, USA
^{bw} University of Texas, Arlington, TX 76019, USA
^{bx} Southern Methodist University, Dallas, TX 75275, USA
^{by} Rice University, Houston, TX 77005, USA
^{bz} University of Virginia, Charlottesville, VA 22901, USA
^{ca} University of Washington, Seattle, WA 98195, USA

ARTICLE INFO

Article history:

Received 20 October 2011
 Received in revised form 11 December 2011
 Accepted 8 January 2012
 Available online 10 January 2012
 Editor: W.-D. Schlatter

ABSTRACT

We present new direct constraints on a general Wtb interaction using data corresponding to an integrated luminosity of 5.4 fb^{-1} collected by the D0 detector at the Tevatron $p\bar{p}$ collider. The standard model provides a purely left-handed vector coupling at the Wtb vertex, while the most general, lowest dimension Lagrangian allows right-handed vector and left- or right-handed tensor couplings as well. We obtain precise limits on these anomalous couplings by comparing the data to the expectations from different assumptions on the Wtb coupling.

Published by Elsevier B.V. Open access under [CC BY license](#).

The top quark was discovered in 1995 at the Tevatron [1,2] via the pair production mode involving strong interactions. In 2009, the electroweak production of the top quark was observed by the D0 and CDF Collaborations [3,4]. At the Tevatron, the dominant production modes for single top quark are the s -channel (“ tb ”) [5] and t -channel (“ tqb ”) [6,7] processes illustrated in Fig. 1. A third process, usually called “associated production” in which the top quark is produced together with a W boson, has a small cross section at the Tevatron compared to the tb and tqb processes [8]. Recently, we presented improved measurements of the single top quark production cross sections [9] and the observation of t -channel single top quark production [10].

The large mass of the top quark implies that it has large couplings to the electroweak symmetry breaking sector of the stan-

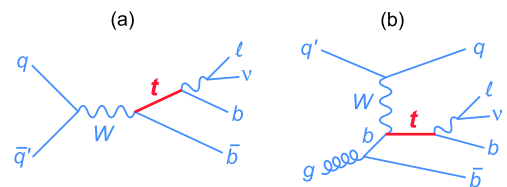


Fig. 1. Tree-level Feynman diagrams for (a) tb and (b) tqb single top quark production.

dard model (SM) and may have non-standard interactions with the weak gauge bosons. Single top quark production provides a unique probe to study the interactions of the top quark with the W boson.

The most general, lowest dimension, CP -conserving Wtb vertex is given by [11]:

$$\mathcal{L} = -\frac{g}{\sqrt{2}} \bar{b} \gamma^\mu (L_V P_L + R_V P_R) t W_\mu^- - \frac{g}{\sqrt{2}} \bar{b} \frac{i\sigma^{\mu\nu} q_\nu}{M_W} (L_T P_L + R_T P_R) t W_\mu^- + \text{h.c.}, \quad (1)$$

where M_W is the mass of the W boson, q_ν is the W boson four-momentum, $P_L = (1 - \gamma_5)/2$ is the left-handed projection operator, $P_R = (1 + \gamma_5)/2$ is the right-handed projection operator,

¹ Augustana College, Sioux Falls, SD, USA.

² The University of Liverpool, Liverpool, UK.

³ UPIITA-IPN, Mexico City, Mexico.

⁴ SLAC, Menlo Park, CA, USA.

⁵ University College London, London, UK.

⁶ Centro de Investigación en Computación – IPN, Mexico City, Mexico.

⁷ ECFM, Universidad Autónoma de Sinaloa, Culiacán, Mexico.

⁸ Universität Bern, Bern, Switzerland.

‡ Deceased.

$L_{V,T} = V_{tb} \cdot f_{L_{V,T}}$ and $R_{V,T} = V_{tb} \cdot f_{R_{V,T}}$. The form factor f_{L_V} (f_{L_T}) represents the left-handed vector (tensor) coupling, f_{R_V} (f_{R_T}) represents the right-handed vector (tensor) coupling, and V_{tb} is the Cabibbo–Kobayashi–Maskawa matrix element. In the SM, the Wtb coupling is left-handed with $L_V \equiv |V_{tb}| \simeq 1$ and $R_V = L_T = R_T = 0$. The magnitudes of the right-handed vector coupling and the tensor couplings can be indirectly constrained by the measured branching ratio of the $b \rightarrow s\gamma$ process [12]. Measurements of top quark decays in $t\bar{t}$ production, e.g. the W boson helicity [13,14], can directly constrain the Lorentz structure of the Wtb vertex [15]. Assuming single top quarks are produced only via W boson exchange, the single top quark cross section is directly proportional to the square of the effective Wtb coupling. Moreover, the event kinematics and angular distributions are also sensitive to the existence of anomalous top quark couplings [16,17]. Therefore, direct constraints on anomalous couplings can be obtained by measuring single top quark production [18].

This analysis uses the same data, event selection, and background modeling as the recent single top quark cross section measurements [9,10]. We perform a study of anomalous Wtb couplings and obtain substantial improvements on the limits of these couplings following the general framework given in Ref. [18]. Out of the four couplings (L_V, L_T, R_V, R_T), we consider three cases pairing the left-handed vector coupling with each of the other three couplings: (L_V, R_V), (L_V, L_T) and (L_V, R_T), and for each case we assume the other two non-SM couplings are negligible. This pairing allows us to limit the complexity of the analysis, while increasing the statistical power and sensitivity for the anomalous coupling under study. We assume that single top quarks are produced exclusively through W boson exchange. Therefore other single top quark production mechanisms, such as flavor-changing neutral current interactions [19,20], the decay of new scalar boson [21], or the exchange of new vector boson [22,23] are not considered here. We also assume that the Wtb vertex dominates top quark production and decay, i.e., $|V_{td}|^2 + |V_{ts}|^2 \ll |V_{tb}|^2$. The results presented here supersede those contained in Ref. [18]. In addition to the analysis of additional data and to the improvements in the event selection and background modeling used for the results presented in Refs. [9,10], we use an updated calculation of the cross section as a function of the anomalous couplings which addresses a mistake present in the original analysis [18] (in that analysis the R_T and L_T couplings were accidentally swapped).

We select single top quark events which are expected to contain exactly one isolated large transverse momentum (p_T) electron or muon and large missing transverse energy (\cancel{E}_T). Events with 2, 3 or 4 jets are selected, and one or two of the jets are required to originate from the hadronization of long-lived b hadrons (b -jets) as determined by a multivariate b -tagging algorithm [24]. To increase the search sensitivity, we divide our data into six independent analysis channels, each with a different background composition and signal-to-background ratio. The channels are based on the number of identified b jets (1 or 2) and jet multiplicity (2, 3 or 4 jets). The signal selection efficiencies with different Wtb couplings, including branching fraction, trigger efficiencies and the b -tagging requirements, vary between 2.7% and 3.0% for tb and 1.9% and 2.2% for tqb production, estimated using Monte Carlo (MC) simulations. The “associated production” process gives a negligible contribution to this analysis.

Single top quark signal events with the SM and anomalous Wtb couplings are modeled using the COMPHEP-based MC event generator SINGLETOP [25] for a top quark mass $m_t = 172.5$ GeV using the CTEQ6M [26] parton distribution functions. The anomalous Wtb couplings are taken into account in both production and decay in the generated samples. The event kinematics for both

s -channel and t -channel processes reproduce distributions from next-to-leading-order calculations [27,28]. The decay of the top quark and the resulting W boson are carried out in the SINGLETOP [25] generator in order to preserve information about the spin of the particles. The theoretical cross sections for anomalous single top quark production ($(s+t)$ -channel) with $|V_{tb}| \simeq 1$ are 3.1 ± 0.3 pb if $f_{R_V} = 1$, 9.4 ± 1.4 pb if $f_{L_T} = 1$ or $f_{R_T} = 1$, and 10.6 ± 0.8 pb if $f_{R_T} = f_{L_V} = 1$ [16]. All other couplings are set to zero when calculating these cross sections. The SM single top quark production cross section is 3.3 ± 0.1 pb [8].

The main background contributions are those from W bosons produced in association with jets ($W + \text{jets}$), $t\bar{t}$ production, and multijet production in which a jet with high electromagnetic content mimics an electron, or a muon contained within a jet originating from the decay of a heavy-flavor quark (b or c quark) appears to be isolated. Diboson (WW, WZ, ZZ) and $Z + \text{jets}$ processes add small additional contributions to the background. The $t\bar{t}$, $W + \text{jets}$, and $Z + \text{jets}$ events are simulated with the ALPGEN leading-log MC generator [29]. The effect of anomalous Wtb couplings on kinematic distributions of the $t\bar{t}$ background has been found to be negligible, thus only SM $t\bar{t}$ samples are considered in the analysis. Diboson processes are modeled using PYTHIA [30]. For all of the signal and background MC samples, PYTHIA is used to simulate parton showers and to model hadronization of all generated partons. The presence of additional $p\bar{p}$ interactions is modeled by events selected from random beam crossings matching the instantaneous luminosity profile in the data. All MC events are processed through a GEANT-based simulation [31] of the D0 detector and reconstructed using the same algorithm as data. Differences between simulation and data in lepton and jet reconstruction efficiencies and resolutions, jet energy scale, and b -tagging efficiencies are corrected in the simulation by applying correction functions measured from separate data samples. The $t\bar{t}$, $Z + \text{jets}$ and diboson MC samples are scaled to their theoretical cross sections [32,33]. We use data containing non-isolated leptons to model the multijet background. $W + \text{jets}$ and multijet backgrounds are normalized by comparing the prediction for background to data before b -tagging. Details of the selection criteria and background modeling are given in Ref. [9].

The main contributions to the systematic uncertainty on the predicted number of events arise from the signal modeling, the jet energy scale (JES), jet energy resolution (JER), corrections to b -tagging efficiency and the correction for jet-flavor composition in $W + \text{jets}$ events. These uncertainties affect the normalization of the distributions, and in some cases (JES, JER, and b -tagging) also change the differential distributions. There are smaller contributions due to limited statistics of the MC samples, uncertainties on the measured luminosity, and the trigger modeling. In addition, we also consider a signal cross section uncertainty (3.8% for tb and 5.3% for tqb) given by the NLO calculation. Details of systematic uncertainties are given in Ref. [9]. Table 1 lists the numbers of events expected and observed for each process as a function of jet multiplicity.

We use a multivariate analysis technique called Bayesian neural networks (BNN) [34] to separate the signal from the backgrounds. The BNN discriminant is trained using the lepton and jets four-vectors, a two-vector for \cancel{E}_T , and variables that include lepton charge and b -tagging information. In addition, four angular variables are added based on top quark spin and W boson helicity information to provide additional discriminating power. The total number of variables used in training for events with 2, 3, and 4 jets is 18, 22, and 26, respectively [9]. Three example distributions from some of the most sensitive variables are shown in Fig. 2: the p_T spectrum of the lepton from the decay of the top quark and the cosine of the angles between

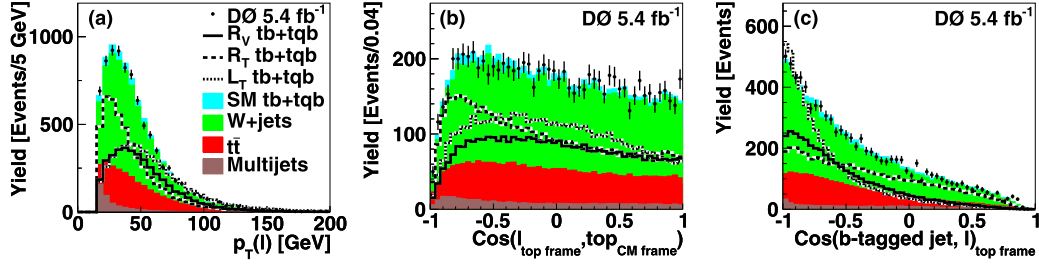


Fig. 2. Comparison of the SM backgrounds and data for selected discriminating variables with all channels combined: (a) lepton p_T , (b) cosine of the angle between the lepton (in the reconstructed top quark frame) and the reconstructed top quark (in the center of mass frame) and (c) cosine of the angle between the leading b -tagged jet and the lepton (both in the reconstructed top quark frame). Superimposed are the distributions from single top quark production (“ $tb + tqb$ ”) with one non-vanishing non-SM coupling (all other couplings set to zero) normalized to 10 times the SM single top quark cross section. The W + jets contributions include the smaller backgrounds from Z + jets and dibosons.

Table 1

Numbers of expected and observed events in 5.4 fb^{-1} of integrated luminosity, with uncertainties including both statistical and systematic components. The single top quark contributions are normalized to their theoretical predictions.

| Source | 2 jets | 3 jets | 4 jets |
|-------------------------------|----------------|----------------|----------------|
| $tb (f_{L_T} = 1)$ | 756 ± 42 | 344 ± 27 | 103 ± 15 |
| $tqb (f_{L_T} = 1)$ | 103 ± 5.8 | 67 ± 6.3 | 28 ± 4.4 |
| $tb (f_{R_V} = 1)$ | 105 ± 6.0 | 43 ± 3.8 | 12 ± 1.9 |
| $tqb (f_{R_V} = 1)$ | 122 ± 7.2 | 61 ± 5.3 | 22 ± 3.7 |
| $tb (f_{R_T} = 1)$ | 730 ± 38 | 316 ± 25 | 92 ± 14 |
| $tqb (f_{R_T} = 1)$ | 117 ± 6.2 | 86 ± 8.6 | 40 ± 5.8 |
| $tb (f_{L_V} = f_{R_T} = 1)$ | 607 ± 31 | 284 ± 21 | 86 ± 13 |
| $tqb (f_{L_V} = f_{R_T} = 1)$ | 268 ± 15 | 167 ± 16 | 67 ± 10 |
| $tb (SM, f_{L_V} = 1)$ | 104 ± 16 | 44 ± 7.8 | 13 ± 3.5 |
| $tqb (SM, f_{L_V} = 1)$ | 140 ± 13 | 72 ± 9.4 | 26 ± 6.4 |
| $t\bar{t}$ | 433 ± 87 | 830 ± 133 | 860 ± 163 |
| W + jets | 3560 ± 354 | 1099 ± 169 | 284 ± 76 |
| Z + jets and dibosons | 400 ± 55 | 142 ± 41 | 35 ± 18 |
| Multijets | 277 ± 34 | 130 ± 17 | 43 ± 5.2 |
| Total SM prediction | 4914 ± 558 | 2317 ± 377 | 1261 ± 272 |
| Data | 4881 | 2307 | 1283 |

the lepton, the leading b -tagged jet and the reconstructed top quark.

For each of the three scenarios, we consider the anomalous coupling sample as the signal when training BNN discriminants: for (L_V, R_V) , the signal is the single top quark sample generated with $f_{R_V} = 1$; for (L_V, R_T) , the signal is the sample generated with $f_{R_T} = 1$; for (L_V, L_T) , the signal is the sample generated with $f_{L_T} = 1$. The background includes the SM single top quark sample with $f_{L_V} = 1$ and all the backgrounds described above. Each background component is represented in proportion to its expected fraction given by the background model. Fig. 3 shows representative BNN discriminant output distributions for the three different scenarios with all six analysis channels combined.

We follow a Bayesian statistical approach [3,35,36] to compare data to the signal predictions given by different anomalous couplings using BNN discriminant output distributions. We compute a two-dimensional (2D) posterior probability as a function of $|V_{tb} \cdot f_{L_V}|^2$ and $|V_{tb} \cdot f_X|^2$, where $V_{tb} \cdot f_X$ is one of the two non-SM couplings $X = \{R_V, L_T\}$. For these two cases the single top quark contribution is represented by a superposition of two samples:

$$s = |V_{tb} \cdot f_{L_V}|^2 s_{L_V} + |V_{tb} \cdot f_X|^2 s_X, \quad (2)$$

where s_{L_V} (s_X) are the mean expected count of single top quarks for the assumptions $f_{L_V} = 1$ ($f_X = 1$) and the other couplings are set to zero. In the (L_V, R_T) scenario, the two couplings interfere, and to account for the effect of the interference, the single top

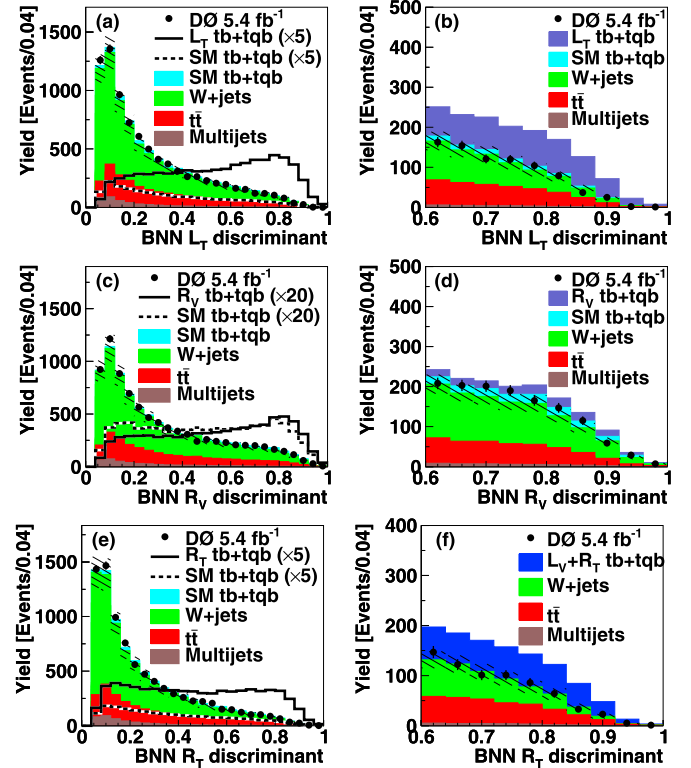


Fig. 3. The left column shows BNN discriminant output distributions of data and of the sum of the SM backgrounds with all channels combined for the whole discriminant range; superimposed are the distributions for the single top quark contributions scaled by (a) 5 times for the (L_V, R_V) scenario, (c) 20 times for the (L_V, R_V) scenario, and (e) 5 times for the (L_V, R_T) scenario. The right column shows BNN discriminant output distributions in the high discriminant region for (b) the (L_V, L_T) scenario, (d) the (L_V, R_V) scenario, and (f) the (L_V, R_T) scenario. The hatched bands give the uncertainty on the background sum. The W + jets contributions include the smaller backgrounds from Z + jets and dibosons.

quark contribution is represented by the superposition of three samples:

$$s = |V_{tb} \cdot f_{L_V}|^2 s_{L_V} + |V_{tb} \cdot f_{R_T}|^2 s_{R_T} + |V_{tb} \cdot f_{L_V}| |V_{tb} \cdot f_{R_T}| (s_{L_V R_T} - s_{L_V} - s_{R_T}), \quad (3)$$

where s_{R_T} is the mean count assuming a left-handed tensor coupling only $f_{R_T} = 1$, and $s_{L_V R_T}$ is the one where both couplings $f_{L_V} = 1$ and $f_{R_T} = 1$. The last sample is indicated as “ $L_V + R_T$ ” in Fig. 3(f). We assume a Poisson distribution for data counts and uniform prior probability for non-negative values of the SM and non-SM couplings. The output discriminants for the signal,

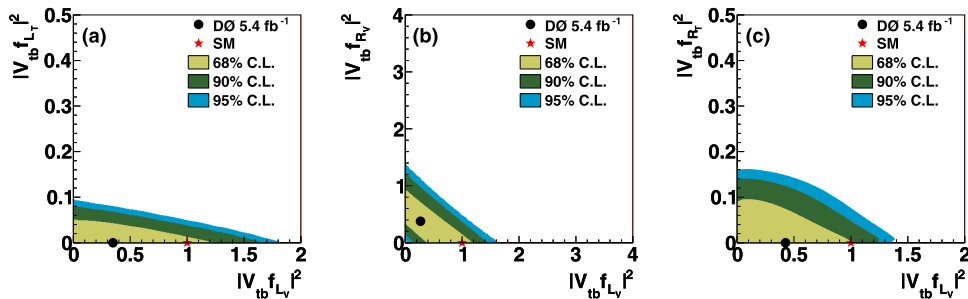


Fig. 4. Two-dimensional posterior probability density distributions for the anomalous couplings. The left row (a) shows the distribution for the (L_V, L_T) scenario, the middle row (b) for the (L_V, R_V) scenario, and the right row (c) for the (L_V, R_T) scenario. The dots represent the peak posterior from our data in comparison with the SM predictions.

Table 2

One-dimensional upper limits at 95% C.L. for anomalous Wtb couplings in the three scenarios.

| Scenario | Cross section | Coupling |
|--------------|---------------|-----------------------------------|
| (L_V, L_T) | < 0.60 pb | $ V_{tb} \cdot f_{L_T} ^2 < 0.06$ |
| (L_V, R_V) | < 2.81 pb | $ V_{tb} \cdot f_{R_V} ^2 < 0.93$ |
| (L_V, R_T) | < 1.21 pb | $ V_{tb} \cdot f_{R_T} ^2 < 0.13$ |

backgrounds, and data are used to form a binned likelihood as a product over all six analysis channels and all bins, taking into account all systematic uncertainties and their correlations. The expected posterior probabilities are obtained by setting the number of data counts to be equal to the predicted sum of the signal and backgrounds.

Fig. 4 shows the 2D posterior probability density distributions for the three scenarios. We do not observe significant deviations from the SM expectations and therefore compute 95% C.L. upper limits on the anomalous couplings by integrating out the left-handed vector coupling to get a one-dimensional posterior probability density. The measured values are given in Table 2. With the SM constraint on the left-handed vector coupling, i.e. $|V_{tb} \cdot f_{L_V}| = 1$, the 95% C.L. limits on left-handed tensor, right-handed vector and tensor couplings are $|V_{tb} \cdot f_{L_T}|^2 < 0.05$, $|V_{tb} \cdot f_{R_V}|^2 < 0.50$ and $|V_{tb} \cdot f_{R_T}|^2 < 0.11$, respectively.

In summary, we have presented a search for anomalous Wtb couplings using 5.4 fb^{-1} of D0 data in the single top quark final state. We find no evidence for anomalous couplings and set 95% C.L. limits on these couplings. These represent improvements in the limits by factors of 2.6 to 5.0 in terms of couplings squared compared to the previous results [18] while a factor of approximately 2.5 is expected from the increase in integrated luminosity. This result represents the most stringent direct constraints on anomalous Wtb interactions.

Acknowledgements

We thank the staffs at Fermilab and collaborating institutions, and acknowledge support from the DOE and NSF (USA); CEA and CNRS/IN2P3 (France); FASI, Rosatom and RFBR (Russia); CNPq, FAPERJ, FAPESP and FUNDUNESP (Brazil); DAE and DST (India); Colciencias (Colombia); CONACyT (Mexico); KRF and KOSEF (Korea); CONICET and UBACyT (Argentina); FOM (The Netherlands); STFC and The Royal Society (United Kingdom); MSMT and GACR (Czech Republic); CRC Program and NSERC (Canada); BMBF and DFG (Germany); SFI (Ireland); The Swedish Research Council (Sweden); and CAS and CNSF (China).

References

[1] F. Abe, et al., CDF Collaboration, Phys. Rev. Lett. 74 (1995) 2626.

- [2] S. Abachi, et al., D0 Collaboration, Phys. Rev. Lett. 74 (1995) 2632.
 [3] V.M. Abazov, et al., D0 Collaboration, Phys. Rev. Lett. 103 (2009) 092001.
 [4] T. Aaltonen, et al., CDF Collaboration, Phys. Rev. Lett. 103 (2009) 092002.
 [5] S. Cortese, R. Petronzio, Phys. Lett. B 253 (1991) 494.
 [6] S.S.D. Willenbrock, D.A. Dicus, Phys. Rev. D 34 (1986) 155.
 [7] C.-P. Yuan, Phys. Rev. D 41 (1990) 42.
 [8] N. Kidonakis, Phys. Rev. D 74 (2006) 114012. The cross sections for the single top quark processes ($m_t = 172.5$ GeV) are 1.04 ± 0.04 pb (s -channel) and 2.26 ± 0.12 pb (t -channel).
 [9] V.M. Abazov, et al., D0 Collaboration, Phys. Rev. D 84 (2011) 112001.
 [10] V.M. Abazov, et al., D0 Collaboration, Phys. Lett. B 705 (2011) 313.
 [11] G.L. Kane, G.A. Ladinsky, C.-P. Yuan, Phys. Rev. D 45 (1992) 124; J.A. Aguilar-Saavedra, Nucl. Phys. B 812 (2009) 181.
 [12] F. Larios, M.A. Perez, C.-P. Yuan, Phys. Lett. B 457 (1999) 334; G. Burdman, M.C. Gonzalez-Garcia, S.F. Novaes, Phys. Rev. D 61 (2000) 114016; B. Grzadkowski, M. Misiak, Phys. Rev. D 78 (2008) 077501; J.P. Lee, K.Y. Lee, Phys. Rev. D 78 (2008) 056004, and references therein.
 [13] V.M. Abazov, et al., D0 Collaboration, Phys. Rev. Lett. 100 (2008) 062004; V.M. Abazov, et al., D0 Collaboration, Phys. Rev. D 83 (2011) 032009.
 [14] A. Abulencia, et al., CDF Collaboration, Phys. Rev. D 73 (2006) 11103; A. Abulencia, et al., CDF Collaboration, Phys. Lett. B 674 (2009) 160; A. Abulencia, et al., CDF Collaboration, Phys. Rev. Lett. 105 (2010) 042002.
 [15] V.M. Abazov, et al., D0 Collaboration, Phys. Rev. Lett. 102 (2009) 092002.
 [16] E. Boos, L. Dudko, T. Ohl, Eur. Phys. J. C 11 (1999) 473.
 [17] D.O. Carlson, E. Malkawi, C.-P. Yuan, Phys. Lett. B 337 (1994) 145; E. Malkawi, C.-P. Yuan, Phys. Rev. D 50 (1994) 4462; A.P. Heinson, A.S. Belyaev, E. Boos, Phys. Rev. D 56 (1997) 3114.
 [18] V.M. Abazov, et al., D0 Collaboration, Phys. Rev. Lett. 101 (2008) 221801.
 [19] V.M. Abazov, et al., D0 Collaboration, Phys. Rev. Lett. 99 (2007) 191802; V.M. Abazov, et al., D0 Collaboration, Phys. Lett. B 693 (2010) 81.
 [20] T. Aaltonen, et al., CDF Collaboration, Phys. Rev. Lett. 102 (2009) 151801.
 [21] V.M. Abazov, et al., D0 Collaboration, Phys. Rev. Lett. 102 (2009) 191802.
 [22] V.M. Abazov, et al., D0 Collaboration, Phys. Lett. B 641 (2006) 423; V.M. Abazov, et al., D0 Collaboration, Phys. Rev. Lett. 100 (2008) 211803; V.M. Abazov, et al., D0 Collaboration, Phys. Lett. B 699 (2011) 145.
 [23] T. Aaltonen, et al., CDF Collaboration, Phys. Rev. Lett. 103 (2009) 041801.
 [24] V.M. Abazov, et al., D0 Collaboration, Nucl. Instrum. Methods Phys. Res. A 620 (2010) 490.
 [25] E.E. Boos, et al., Phys. Atom. Nucl. 69 (2006) 1317. We use SINGLETOP version 4.2p1.
 [26] J. Pumplin, et al., J. High Energy Phys. 0207 (2002) 012. We use versions CTEQ6M for signal and CTEQ6L1 for background.
 [27] Z. Sullivan, Phys. Rev. D 70 (2004) 114012.
 [28] J.M. Campbell, R. Frederix, F. Maltoni, F. Tramontano, Phys. Rev. Lett. 102 (2009) 182003.
 [29] M.L. Mangano, et al., J. High Energy Phys. 0307 (2003) 001. We use ALPGEN version 2.11.
 [30] T. Sjöstrand, S. Mrenna, P. Skands, J. High Energy Phys. 0608 (2006) 026. We use version 6.409.
 [31] R. Brun, F. Carminati, CERN Program Library Long Writeup, Report No. W5013, 1993.
 [32] S. Moch, P. Uwer, Phys. Rev. D 78 (2008) 034003. At $m_t = 172.5$ GeV, $\sigma(p\bar{p} \rightarrow t\bar{t} + X) = 7.46$ pb.
 [33] R.K. Ellis, Nucl. Phys. B (Proc. Suppl.) 160 (2006) 170. We use MCFM version 5.1.
 [34] R.M. Neal, Bayesian Learning for Neural Networks, Springer-Verlag, New York, 1996.
 [35] V.M. Abazov, et al., D0 Collaboration, Phys. Rev. Lett. 98 (2007) 181802.
 [36] V.M. Abazov, et al., D0 Collaboration, Phys. Rev. D 78 (2008) 012005.